Strain-induced effects in colloidal quantum dots: lifetime measurements and blinking statistics

2010 Nanotechnology 21 134024

(http://iopscience.iop.org/0957-4484/21/13/134024)

Nanotechnology **21** (2010) 134024 (6pp) doi:10.1088/0957-4484/21/13/134024

Strain-induced effects in colloidal quantum dots: lifetime measurements and blinking statistics

V Veilleux[1], D Lachance-Quirion[1], K Doré[2], D B Landry[1], P G Charette[3] and C Nì Allen[1]

[1] Centre d'optique, photonique et laser (COPL), 2375 rue de la Terrasse, Université Laval, QC, G1V 0A6, Canada
[2] Centre de Recherche Université Laval Robert-Giffard (CRULRG), 2601, de la Canardière, QC, G1J 2G3, Canada
[3] Centre d'optique, photonique et laser (COPL), Université de Sherbrooke, Sherbrooke, J1K 2R1, Canada

E-mail: claudine.allen@phy.ulaval.ca

Received 31 August 2009, in final form 29 October 2009
Published 8 March 2010
Online at stacks.iop.org/Nano/21/134024

Abstract
A series of samples of CdSe/$Cd_xZn_{1-x}S$ core/shell quantum dots have been synthesized in order to measure the influence of lattice-mismatch-induced strain on the photoluminescence (PL) and blinking behaviour. The PL spectra show a significant variation of the fluorescence wavelength even though the colloidal quantum dots (cQDs) are similar in size. The PL excitation spectra show a gradual splitting of the first exciton level as the proportion of Zn is increased in the shell and as the shell grows. On the other hand, blinking studies clearly demonstrate a significant dependence on the amount of Zn present in the shell. Distributions of on and off times go from the usual power-law distributions to power-law distributions with exponential cut-offs. These cut-offs become increasingly pronounced as the proportion of Zn increases. We interpret these results in the framework of diffusion-controlled electron transfer. Exciton relaxation lifetime measurements strongly suggest that lattice mismatch is responsible for a greater number of defects in core/shell cQDs. Therefore, strain and lattice mismatch are shown to be parameters of significant importance for the electronic structure of nanocrystals, influencing the photoluminescence, exciton relaxation lifetime and blinking behaviour.

1. Introduction

Colloidal quantum dots (cQDs) represent an exciting opportunity for applications in new devices and new areas such as single-molecule tracking [1], light-emitting devices [2] and so on. The interest of cQDs lies in the ability to easily tune the light emission properties by varying the synthesis parameters. Indeed, their small size (a few nanometres) creates a quantum confinement of the excitons, thus decreasing the emission wavelength relative to the bandgap of the bulk materials used.

To further enhance their emission properties, studies have shown [3] that one can grow a shell of a higher bandgap semiconductor around the nanocrystal from one to several monolayers thick [4, 5]. This has been shown to significantly improve the photoluminescence of the cQDs and to suppress the blinking with very thick [6] or multiple nearly lattice-matched shells [7]. Although these enhancements are very desirable, until recently [8, 9] little attention had been paid to the compatibility of the lattice parameters between the core and shell in cQDs. Indeed, the lattice mismatch between successive layers is a crucial parameter in MOCVD and MBE growth as it can, if too high, lead to defects and dislocations [10]. These defects, acting as charge carrier traps, have been highlighted as a potential cause for blinking, which plagues colloidal QDs while being almost nonexistent in their epitaxial counterparts [11]. So here, by designing shell-alloy samples with a gradually varying lattice mismatch, we show that strain is an important factor for colloidal semiconductor nanocrystals as it influences the spectral characteristics, the exciton relaxation lifetimes and the blinking behaviour of

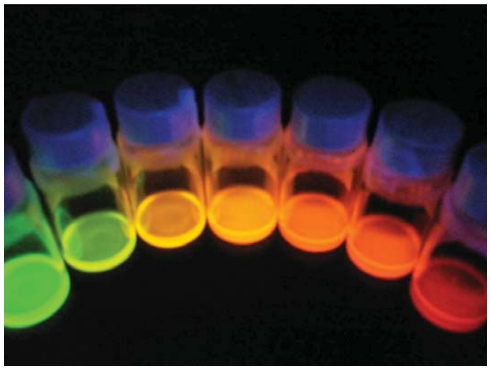

Figure 1. The PL of $Cd_xZn_{1-x}S$ shell-alloy samples seen under UV light excitation. The proportion of Cd grows from left ($x = 0$) to right ($x = 1$).

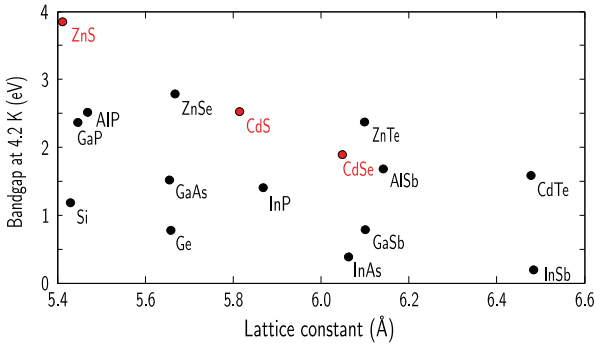

Figure 2. Low-temperature bandgap energies versus lattice constants of chosen semiconductors. Data taken from [10]. In red, semiconductors used in the making of the shell-alloy samples.

cQDs. We emphasize the effect of the shell alloy, with its related lattice-mismatch-induced strain, on the blinking probability distributions. We interpret these in the framework of diffusion-controlled electron transfer (DCET) [12, 13] and show a novel dependence of the exponential cut-off on lattice mismatch.

2. Experimental details

2.1. Sample synthesis

To better understand how strain affects the properties of cQDs, a series of CdSe core samples have been prepared with $Cd_xZn_{1-x}S$ shell alloys (see figure 1) using the successive ion layer adsorption and reaction method (SILAR) [4, 5]. This method allows to adjust the synthesis parameters in order to grow a seven-monolayer shell, grown one layer at a time, on the CdSe cores in each sample. By tuning the amount of precursors of ZnS and CdS added to form the shell, one can achieve a shell alloy of any given Cd:Zn proportion. It should be noted that, as has been previously reported for capped cQDs [3], these shell-alloy cQDs are all more luminescent than CdSe cores since their surfaces are better passivated. All samples were synthesized from the same monodisperse CdSe cores (average diameter 3.1 nm). Since ZnS and CdSe have a lattice mismatch of 12% whereas CdS and CdSe lattices differ by only 3.9%, these samples have a gradually varying lattice mismatch. It must also be mentioned that the shell bandgap increases with increasing Zn going from ∼2.5 to ∼4 eV at liquid helium temperature (see figure 2).

2.2. PL and PLE spectra

Photoluminescence spectra were obtained from ensembles of cQDs in acrylic optical cuvettes. The samples were illuminated with a 15 mW argon-ion laser at 488 nm. The PL was then coupled into a multi-mode optical fibre and into an Ocean Optics USB4000 visible spectrometer.

Photoluminescence excitation (PLE) spectra were performed using a standard spectrofluorimeter (Jobin-Yvon) where the detection wavelength was fixed at the maximal PL emission intensity and the excitation was scanned over the visible spectrum. For every sample, the signal was accumulated for 0.3 s and the resulting spectra have a 1 nm resolution.

2.3. Lifetime measurements

Lifetime measurements were performed using a fluorescence lifetime imaging microscope (FLIM). Samples mounted in Prolong Gold (Invitrogen) were illuminated with a Chameleon Ultra IR laser (Coherent) at 80 MHz repetition rate tuned at 800 nm for two-photon excitation. Fluorescence emission was detected with a cooled high speed PMT detector head (PMC-100-1, Becker and Hickl, Germany) between 380 and 750 nm by means of a multiphoton emission filter (FF01-750/SP-25, Semrock). The acquisition of fluorescence lifetimes was synchronized by a time-correlated-single-photon-counting (TCSPC) module (SPC-830, Becker and Hickl, Germany). Measurements were performed on a Zeiss LSM 510 microscope using a 63× water-immersion objective. Fluorescence decays were analysed with SPCimage (Becker and Hickl).

2.4. Blinking measurements

The shell-alloy samples were diluted and then deposited on properly cleaned glass coverslips. In order to ensure the best possible dispersion of cQDs on the glass substrates and to avoid aggregates, each shell-alloy sample was previously placed in an ultrasonic bath, precipitated twice in isopropanol and then resuspended in hexanes. This last step serves to remove excess ligands and octadecene in solution.

To collect the PL from individual shell-alloy cQDs, an Olympus IX71 fluorescence microscope was used with an Olympus 100X oil-immersion 1.3 NA objective. The excitation source was an Exfo X-Cite white lamp going through a blue excitation filter, a dichroic mirror and an orange emission filter mounted on a dichroic cube (Semrock filter sets). The signal from single cQDs was then recorded using a fast EMCCD camera (Andor i-Xon EM + 860). Time traces of several single cQDs were obtained for each sample with 2 ms time bins (500 Hz). The time traces extend from 2 ms to a few

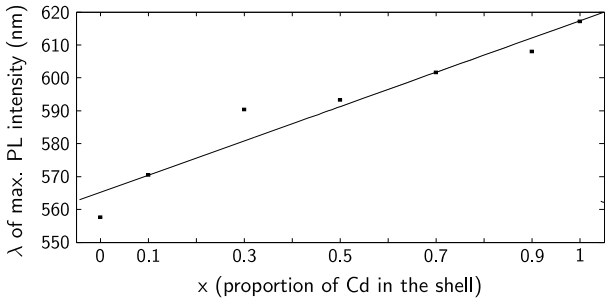

Figure 3. Wavelength (λ) of maximal photoluminescence intensity as a function of the proportion of Cd in the $Cd_xZn_{1-x}S$ shell. The cQDs progressively emit at higher energy as both the effective bandgap of the shell and the strain increase. The emission goes from red to green, covering a range of approximately 60 nm.

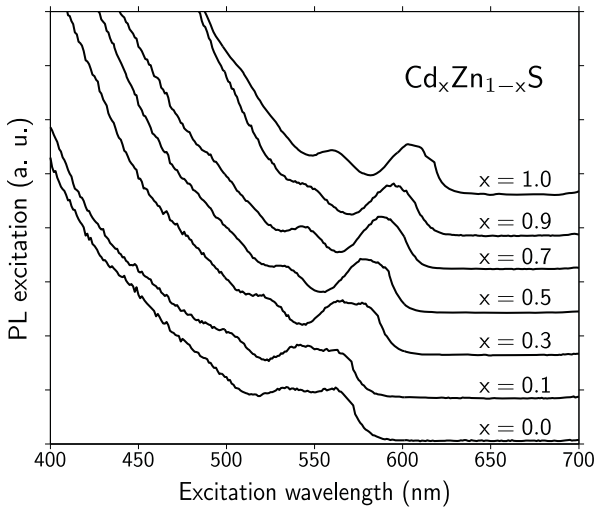

Figure 4. PL excitation spectra for seven $Cd_xZn_{1-x}S$ shell-alloy cQD samples. As the proportion of Zn grows, the first exciton peak gradually splits.

seconds ensuring that the resulting probability distributions are statistically significant.

The emission intensity for each of several cQDs has been recorded and a threshold analysis was performed in order to retrieve the on- and off-time distributions. The threshold was chosen as the midpoint between the maximal and minimal intensity value recorded for a given sequence. Then, the time trace is made binary by setting every intensity value as on (off) when it is above (below) the threshold. It is worth noting that single cQDs that remained on for the whole sequence were rejected as it is impossible to tell whether it is an aggregate or not. Obviously, those remaining off for the whole sequence are simply not detected.

3. Results and discussion

3.1. Spectral characteristics

In order to better probe the behaviour of the charge carriers inside and at the surface of cQDs, we gathered spectral information for each shell-alloy cQD sample. We found that the Cd:Zn ratio has a significant influence on the PL and PLE spectra. As we can see in figure 3, the maxima of the emission spectra are blue-shifted as more Zn is present in the shell. Two factors could contribute to this relative blue-shift with increased Zn proportion: (1) deeper confinement potentials keep the charge carriers more localized in the core, hence their wavefunctions are less spread out with corresponding higher energy states, and (2) the core is under more compressive strain due to the increasing core/shell lattice mismatch, thus the resulting deformation potentials affecting the CdSe band structure increase its energy bandgap [14]. However, the second factor could be partially compensated by the tensile strain in the shell, but its deformation should be smaller because the shell alloys are more mechanically stiff [14]. It should also be noted that the physical size of the core/shell cQDs is not likely to play a significant role as TEM images have shown that all the samples have similar diameters [16].

The shift seen in figure 3 is also visible in the PLE spectra (figure 4) where one can notice a splitting of the first exciton peak into two distinct peaks. This behaviour is reminiscent of lifting energy state degeneracies with an anisotropic perturbation. Since the growth conditions were chosen such that all cQD samples would roughly keep their spherical symmetry, we suggest that an anisotropy of the strain field increasing with lattice mismatch is the cause of the observed splitting. It has recently been shown that non-hydrostatic pressure of a few GPa applied externally on CdSe/CdS cQDs can indeed split the exciton ground states [15]. Internal pressures above 1 GPa in core/shell cQDs can be easily reached with a lattice mismatch of a few per cent [17]. The origin of the anisotropy in our cQDs is their dominantly wurtzite phase with different lattice mismatches, hence strains, occurring on different crystallographic planes. More details about spectral characterizations can be found elsewhere [16].

3.2. Lifetime measurements

For every shell-alloy sample, the measured lifetimes were best fitted either to a single exponential or to a sum of two exponentials. For every shell-alloy sample, the long-lifetime dynamic associated to the relaxation of the exciton ground state is presented in figure 5. Through the well-known formula $\tau = (\gamma_R + \gamma_{NR})^{-1}$ [18], we see that either changes in radiative or non-radiative recombination mechanisms, with associated rates γ_R and γ_{NR} respectively, can lead to a shorter excited state lifetime (τ). If the changes in γ_{NR} with the Cd:Zn ratio are assumed to be the dominant contribution for the behaviour of τ in the first place, two factors should be considered to explain the observations. On one hand, relaxation of the lattice-mismatch-induced strain by creation of structural defects within the cQDs provide more possibilities for non-radiative recombination, which would decrease the lifetime when the proportion of Zn increases. On the other hand, CdS having a smaller bandgap than ZnS, the charge carriers' wavefunctions are less confined when the proportion of Cd

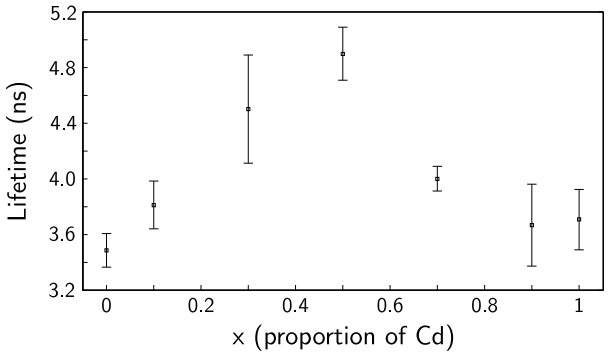

Figure 5. Exciton lifetime (τ) measurements for seven $Cd_xZn_{1-x}S$ shell-alloy cQD samples. The error bars represent the standard deviation for at least ten different measurements for each sample.

increases and can more freely tunnel to surface traps. This again leads to shorter lifetimes since these traps also provide more non-radiative recombination channels. In the second place, if the changes in γ_R are considered significant, one must examine how the electron and hole wavefunction overlap vary with the Cd:Zn ratio. A previous report on a model of CdSe/CdS showed significant delocalization of the electron wavefunction in the shell while the hole wavefunctions stay confined in the core [14]. The overlap could thus be expected to decrease with more Cd in the shell, hence decreasing γ_R and lengthening the lifetimes τ. This is consistent with the first four data points on the left of figure 5, but the drop in lifetime for the last three points on the right seems to correspond only to a large contribution of non-radiative recombination channels that could be provided by surface states as mentioned before.

3.3. Blinking statistics

In the past few years, a number of models have been proposed in order to explain the blinking of single cQDs [12, 13, 19–23]. A few review articles show the differences between these models [24–26]. To discriminate between these numerous models, several studies have sought a dependence between the blinking statistics and synthesis parameters (presence of a shell [20], thickness of the shell [6, 7], ...) and environmental factors (temperature, excitation intensity [20], pH [27], substrate nature [28], ...). These studies have focused on finding the underlying mechanism(s) for blinking and, among other goals, have tried to figure out if it is caused by the surface/environment. Evidence is still somewhat conflicting on this issue. Among other characteristic features, one of the most striking feature of blinking is an apparently universal power-law distribution of on and off times. A characteristic exponent of the behaviour hovering around $-3/2$ has been observed for the first time in [29] and has been frequently observed since then. Authors have reported this behaviour not only for cQDs, but also in other types of emitters, namely nanorods, single fluorescent molecules, polymer segments and fluorescent proteins [24, 25]. In cQDs, the reported characteristic exponents vary from -1.1 to -2.2, averaging around $-3/2$ [24]. Even though these probability distributions

Table 1. Fitting parameters for every shell-alloy sample. The on- and off-time distribution are fitted to $P(t) = at^{-\mu}e^{-\Gamma t}$. The absence of parameter Γ indicates that the distribution is better fitted with only a usual power law ($\Gamma = 0$).

Sample	μ_{on}	Γ_{on}	μ_{off}	Γ_{off}
ZnS	0.86	33	0.63	88
$Cd_{0.1}Zn_{0.9}S$	0.65	47	0.53	74
$Cd_{0.3}Zn_{0.7}S$	1.1	20	1.4	19
$Cd_{0.5}Zn_{0.5}S$	1.1	20	1.6	17
$Cd_{0.7}Zn_{0.3}S$	1.6	15	1.8	11
$Cd_{0.9}Zn_{0.1}S$	1.9	14	1.8	—
CdS	1.8	—	2.0	—

extend over many orders of magnitude in time, an exponential cut-off is often observed for the on times and is postulated to happen on a longer timescale for off times [30].

The distributions of on and off times for our seven $Cd_xZn_{1-x}S$ shell-alloy cQDs are presented in figure 6. The distributions are fitted to a power law with exponential cut-off, explicitly, $P(t) = at^{-\mu}e^{-\Gamma t}$. The parameters of the fitted curves are shown in table 1. We can see that, for $x = 1$, both distributions are power-law distributions. This behaviour evolves and, as the parameter x is lowered, the power-law exponents become smaller and the cut-offs become more pronounced.

We interpret these results in the framework of DCET [12, 13] as it naturally explains exponential cut-offs and can accommodate a range of power-law exponents other than $-3/2$. In the DCET theory, the exponential cut-offs (Γ_k) are given in terms of other physical parameters of the model, namely

$$\Gamma_k = \frac{E_{a,k}}{2\tau_k K_B T}, \qquad k = \text{on, off}, \tag{1}$$

where τ_k is the diffusion time constant, K_B is the Boltzmann constant and $E_{a,k}$ is linked to the energy difference between the two parabolic surface potentials between which diffusion occurs [12, 13]. Given this expression, at a constant temperature, the general decreasing trend of the exponential cut-offs observed along the shell-alloy series with increasing x values must be explained either by a change in $E_{a,k}$ or τ_k. A reasonable hypothesis could then be that more defects in the structure increases the availability of trap states and effectively lowers the diffusion time constants.

Even though the characteristic exponents of the distribution, especially for the higher Zn proportions, depart significantly from the typical blinking behaviour, we can nevertheless see a clear trend of decreasing power-law exponent with increasing Zn proportion. According to [13], DCET could accommodate a power-law behaviour other than $-3/2$ by considering a non-Markovian diffusion process. Our results thus suggest that such an extension is required in order to completely explain the blinking behaviour of shell-alloy cQDs.

4. Conclusions

cQDs have been synthesized with a gradually varying shell alloy. This has allowed to systematically assess the effect

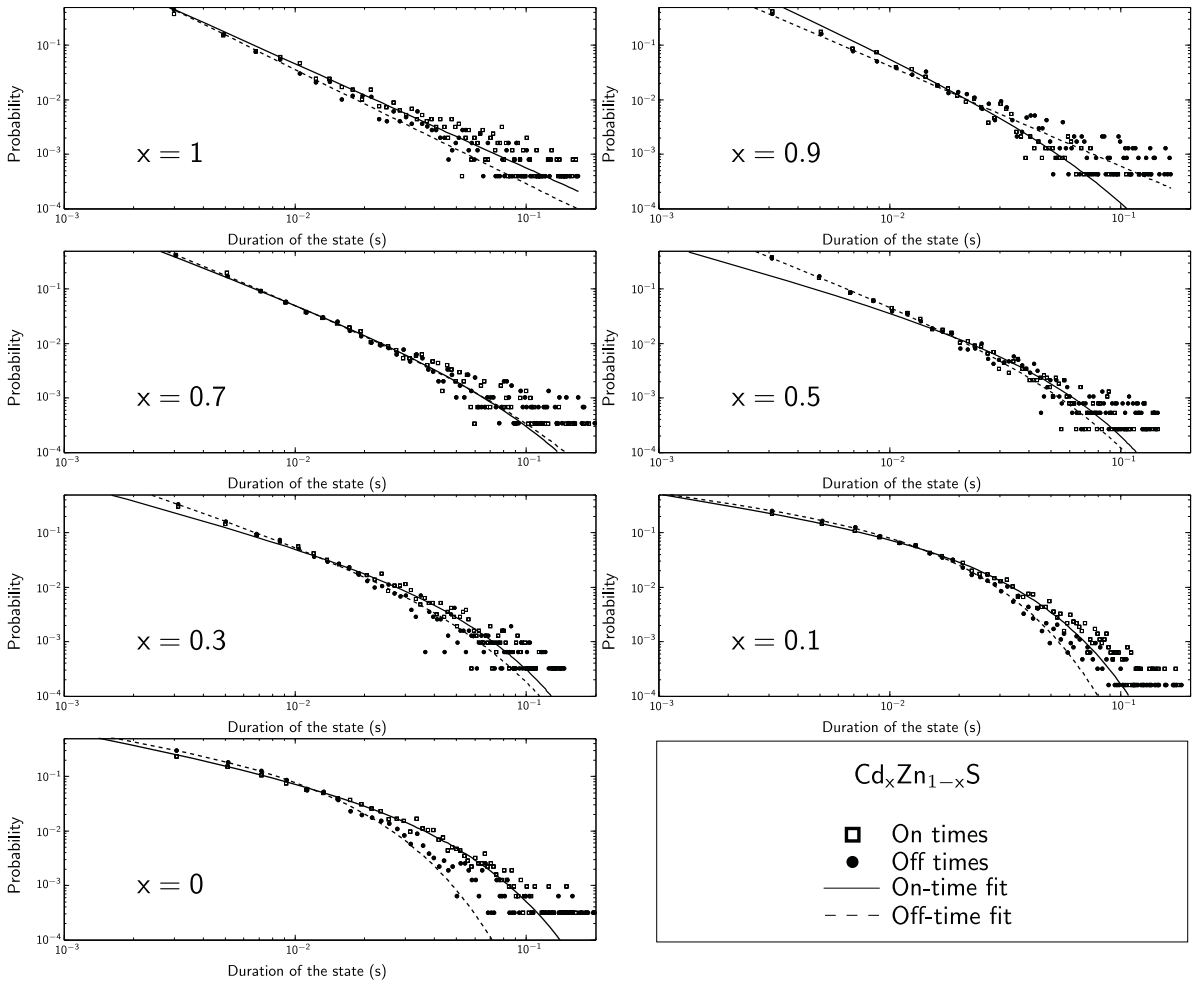

Figure 6. On- and off-time distributions for seven $Cd_xZn_{1-x}S$ shell-alloy cQD samples. Both on- and off-time distributions are fitted to a power-law distribution with exponential cut-off ($P(t) = at^{-\mu}e^{-\Gamma t}$). As the proportion of Zn grows the cut-off gets steeper and the deviation from the power-law behaviour is increasingly obvious. The fitted parameters μ and Γ are shown in table 1.

of lattice mismatch in core/shell cQDs. This parameter was found to significantly alter the spectral measurements, the exciton relaxation lifetimes as well as the blinking behaviour of the shell-alloy samples. Energy level splitting was noted in PLE spectra showing that the electronic configuration is deeply altered by the nature of the shell, most likely via the anisotropic strain field of lattice-mismatched cQDs. Exciton relaxation lifetimes are equally affected by structural defects of the nanocrystal and by the height of the confinement (bandgap of the shell) leading to a maximal exciton relaxation lifetime in the middle of the series for CdSe/$Cd_{0.5}Zn_{0.5}S$ and to minima at the extremes. Lastly, blinking distributions show a power-law behaviour with an exponential cut-off that becomes more pronounced with increased Zn proportion. This behaviour, could possibly be interpreted in terms of an extension of the DCET theory. The fact that exciton relaxation lifetimes and exponential cut-offs do not follow the same trend with increasing lattice mismatch underlines the subtlety of the effect of strain in core/shell nanocrystals.

Acknowledgments

The authors would like to thank M Gauthier for precious help and advice with the blinking experimental setup, P Larochelle for technical assistance and O Voznyy for helpful discussions. VV thanks FQRNT and CNA thanks NSERC for providing funds for this research.

References

[1] Michalet X, Pinaud F F, Bentolila L A, Tsay J M, Doose S, Li J J, Sundaresan G, Wu A M, Gambhir S S and Weiss S 2005 Quantum dots for live cells, *in vivo* imaging, and diagnostics *Science* **307** 538–44

[2] Caruge J M, Halpert J E, Wood V, Bulovic V and Bawendi M G 2008 Colloidal quantum-dot light-emitting diodes with metal-oxide charge transport layers *Nat. Photon.* **2** 247–50

[3] Hines M A and Guyot-Sionnest P 1996 Synthesis and characterization of strongly luminescing ZnS-capped CdSe nanocrystals *J. Phys. Chem.* **100** 468–71

[4] Jack J, Li Y, Wang A, Guo W, Keay J C, Mishima T D, Johnson M B and Peng X 2003 Large-scale synthesis of

nearly monodisperse CdSe/CdS core/shell nanocrystals using air-stable reagents via successive ion layer adsorption and reaction *J. Am. Chem. Soc.* **125** 12567–75

[5] Xie R, Kolb U, Li J, Basche T and Mews A 2005 Synthesis and characterization of highly luminescent CdSe-core CdS/Zn0.5Cd0.5S/ZnS multishell nanocrystals *J. Am. Chem. Soc.* **127** 7480–8

[6] Mahler B, Spinicelli P, Buil S, Quelin X, Hermier J-P and Dubertret B 2008 Towards non-blinking colloidal quantum dots *Nat. Mater.* **7** 659–64

[7] Chen Y, Vela J, Htoon H, Casson J L, Werder D J, Bussian D A, Klimov V I and Hollingsworth J A 2008 'Giant' multishell CdSe nanocrystal quantum dots with suppressed blinking *J. Am. Chem. Soc.* **130** 5026–7

[8] Smith A M, Mohs A M and Nie S 2009 Tuning the optical and electronic properties of colloidal nanocrystals by lattice strain *Nat. Nano* **4** 56–63

[9] Wang X, Ren X, Kahen K, Hahn M A, Rajeswaran M, Zacher S M, Silcox J, Cragg G E, Efros A L and Krauss T D 2009 Non-blinking semiconductor nanocrystals *Nature* **459** 686–9

[10] Yu P Y and Cardona M 2005 *Fundamentals of Semiconductors* (Berlin: Springer)

[11] Pistol M-E, Castrillo P, Hessman D, Prieto J A and Samuelson L 1999 Random telegraph noise in photoluminescence from individual self-assembled quantum dots *Phys. Rev.* B **59** 10725–9

[12] Tang J and Marcus R A 2005 Diffusion-controlled electron transfer processes and power-law statistics of fluorescence intermittency of nanoparticles *Phys. Rev. Lett.* **95** 107401

[13] Tang J and Marcus R A 2005 Mechanisms of fluorescence blinking in semiconductor nanocrystal quantum dots *J. Chem. Phys.* **123** 054704–12

[14] Pandey A and Guyot-Sionnest P 2007 Intraband spectroscopy and band offsets of colloidal II–VI core/shell structures *J. Chem. Phys.* **127** 104710–10

Adachi S 2005 *Properties of Group-IV, III-V and II-VI Semiconductors* (Chichester: Wiley)

[15] Choi C L, Koski K J, Sivasankar S and Alivisatos A P 2009 Strain-dependent photoluminescence behavior of CdSe/CdS nanocrystals with spherical, linear, and branched topologies *Nano Lett.* **9** 3544–9

[16] Allen C Nì *et al* 2009 Manipulating the optoelectronic properties of CdSe colloidal quantum dots using a $Zn_xCd_{1-x}S$ alloyed shell, at press

[17] Ithurria S, Guyot-Sionnest P, Mahler B and Dubertret B 2007 Mn^{2+} as a radial pressure gauge in colloidal core/shell nanocrystals *Phys. Rev. Lett.* **99** 265501–4

[18] Lakowicz J R 2006 *Principles of Fluorescence Spectroscopy* (Berlin: Springer)

[19] Efros A L and Rosen M 1997 Random telegraph signal in the photoluminescence intensity of a single quantum dot *Phys. Rev. Lett.* **78** 1110

[20] Shimizu K T, Neuhauser R G, Leatherdale C A, Empedocles S A, Woo W K and Bawendi M G 2001 Blinking statistics in single semiconductor nanocrystal quantum dots *Phys. Rev.* B **63** 205316

[21] Verberk R, van Oijen A M and Orrit M 2002 Simple model for the power-law blinking of single semiconductor nanocrystals *Phys. Rev.* B **66** 233202

[22] Margolin G and Barkai E 2005 Nonergodicity of blinking nanocrystals and other Lévy-Walk processes *Phys. Rev. Lett.* **94** 080601

[23] Frantsuzov P A and Marcus R A 2005 Explanation of quantum dot blinking without the long-lived trap hypothesis *Phys. Rev.* B **72** 155321

[24] Cichos F, von Borczyskowski C and Orrit M 2007 Power-law intermittency of single emitters *Curr. Opin. Colloid Interface Sci.* **12** 272–84

[25] Frantsuzov P, Kuno M, Janko B and Marcus R A 2008 Universal emission intermittency in quantum dots, nanorods and nanowires *Nat. Phys.* **4** 519–22

[26] Efros A L 2008 Nanocrystals: almost always bright *Nat. Mater.* **7** 612–3

[27] Durisic N, Wiseman P W, Grutter P and Heyes C D 2009 A common mechanism underlies the dark fraction formation and fluorescence blinking of quantum dots *ACS Nano* **3** 1167–75

[28] Shimizu K T, Woo W K, Fisher B R, Eisler H J and Bawendi M G 2002 Surface-enhanced emission from single semiconductor nanocrystals *Phys. Rev. Lett.* **89** 117401

[29] Kuno M, Fromm D P, Hamann H F, Gallagher A and Nesbitt D J 2000 Nonexponential blinking kinetics of single CdSe quantum dots: a universal power law behavior *J. Chem. Phys.* **112** 3117–20

[30] Chung I and Bawendi M G 2004 Relationship between single quantum-dot intermittency and fluorescence intensity decays from collections of dots *Phys. Rev.* B **70** 165304